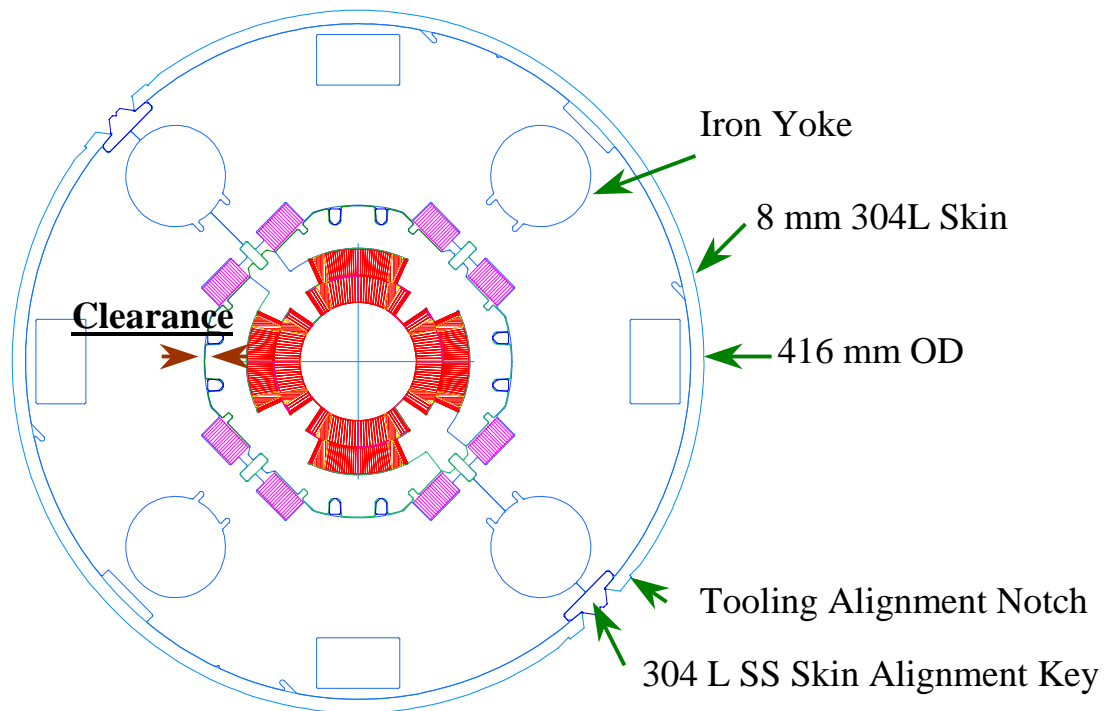


# MQXB Longitudinal Weld Analysis: Part - I

**Deepak Chichili and Jim Kerby**  
*Engineering and Fabrication Department*  
*Technical Division*  
*Fermilab*  
*Batavia, IL 60510*

## 1.0 COLD MASS DESIGN REVIEW

The mechanical support for the coil assembly is entirely provided by the Nitronic 40 collar structure in the straight section and the G-11/aluminum collet assembly in the end regions. The iron yoke is merely for the flux return and the 304 L stainless steel skin is used to hold the two iron halves together. The skin also acts as a helium vessel. Fig. 1 shows the cross-section of the cold mass. The collared coil assembly is placed inside the yoke using four alignment keys. Note that there is a clearance between the collared coil assembly and the yoke inner radius.



**Figure 1:** *MQXB Cold Mass Assembly.*

The two halves of the skin are welded on to a 304 L stainless steel alignment key using an automated TIG welding process. The filler material is 308 L austenitic steel. By design the skin and the alignment key combination have a longer at rest perimeter than the yoke halves. Fig. 2 shows the mechanical model yoke-skin assembly just before welding. Note the gap between the yoke and the skin. It requires 5 weld passes to fill the weld groove and

the weld shrinkage is monitored after each pass. Fig. 3 shows the weld shrinkage along the length of the magnet after each weld pass. Note the total weld shrinkage is about 3 mm which is exactly the gap left between the yoke and the skin before the welding. Thus the skin just touches the yoke assembly after welding. Hence we expect the skin stress after welding to be close to zero. However the skin stress increases during cooldown due to differential thermal contraction and was estimated to be about 200 MPa. If there is an excess in weld shrinkage the skin stress after cool down was computed using FEA with contact frictional elements between yoke and the skin with coefficient of friction of 0.1 [1]. The stress in the skin after cooldown was found to be about 300 MPa for 0.15 mm in excess of weld shrinkage.

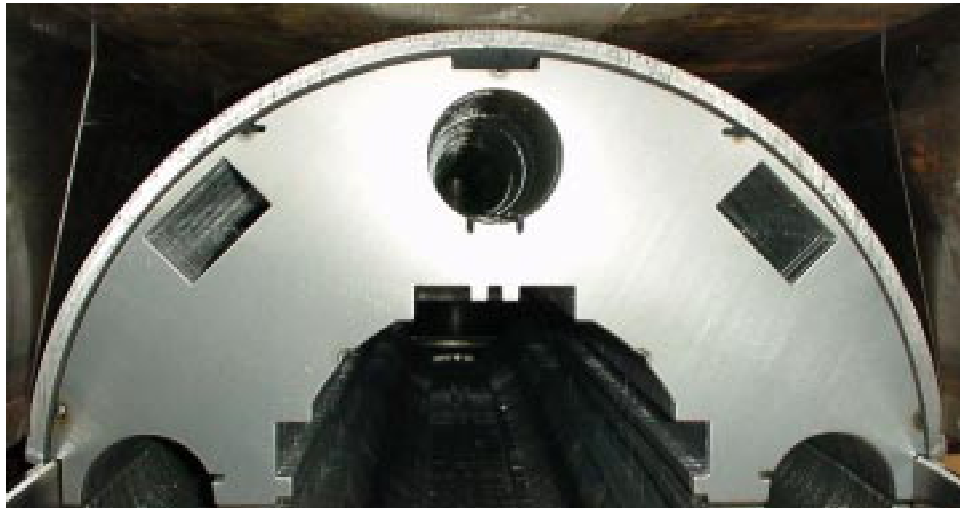


**Figure 2:** Upper Yoke - Skin assembly before welding.

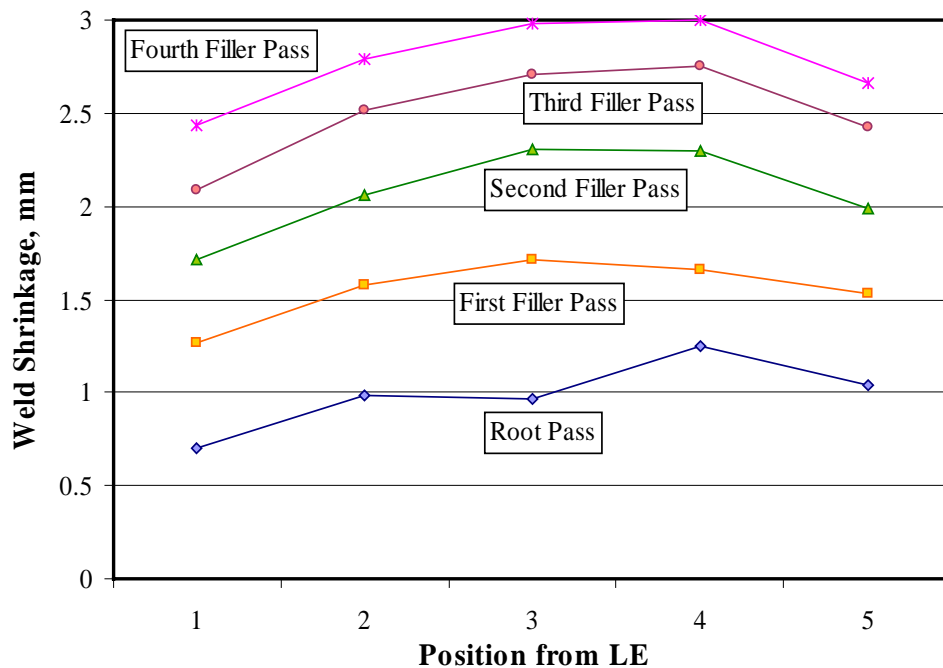


**Figure 3:** Weld Shrinkage after each weld pass along the length of the mechanical model.

## 2.0 BACKGROUND INFORMATION

### (a) Filler Materials:

BNL/NIST reviewed the effect of each constituent elements on the fracture toughness and the strength of the weldments for cryogenic applications [2]. The following summarizes their findings:

#### Delta Ferrite:

The ferrite phase occurs when the composition is adjusted so that the austenite phase is metastable. A small amount of ferrite is normally desirable in stainless steel welds, because it inhibits the formation of low melting point compounds that promote hot cracking in fully austenitic alloys. However for the best toughness in cryogenic applications ferrite content should be minimized.

#### Nitrogen:

Siewert et al. [3] at NIST performed tension tests on 316 LN welds with varying nitrogen content at 298, 76 and 4 K. They observed an increase in strength with increase in nitrogen content and this strengthening effect was more apparent as temperature decreases. The upper limit of N is determined by its solubility in the microstructure above which weld porosity results. Mn is used to enhance the solubility limit of N by providing greater protection from porosity formation.

#### Nickel:

Nickel improves the fracture toughness of the welds by reducing the ferrite content. It also stabilizes the austenitic structure against the formation of martensite during the deformation of the structure.

#### Oxygen:

Oxygen combines with other elements in the welds to form oxide inclusion. These inclusions inhibit dislocations thus forming stress concentration sites which lead to the void formation [4]. Thus reducing oxide inclusions reduces propensity for void formation which then increases the toughness of the weld. McCowan et al. [4] found that the fracture toughness of 316L welds with GMAW process increased with increasing average inclusion spacing or decreasing inclusion density.

Kim et al. [5] studied the effect of oxygen and ferrite content on cryogenic toughness of austenitic stainless steel welds. Their tests showed that there are combinations of oxygen and ferrite contents in the weld metal that could meet ASME requirement of 0.38 mm lateral expansion and that the recommended ferrite content becomes smaller as the oxygen content of the weld increases. Fig. 4 shows the test results. Their results indicate that the low oxygen weld like GTAW (shown with arrows) can meet the ASME requirement quite safely even with a relatively high ferrite content while the high oxygen weld cannot even with a low ferrite content of 5%. Therefore, the ASME recommendation to have 3 FN seems to be reasonable for the weldments other than GTAW.

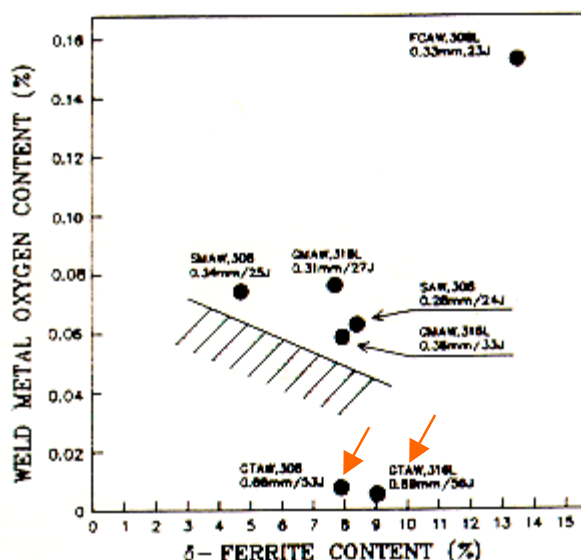


**Figure 4:** The effect of oxygen and ferrite contents on the 77 K lateral expansion [5].

Note that BNL used gas metal arc welding (GMAW) for RHIC magnets whereas Fermilab will be using gas tungsten arc welding (GTAW) process for MQXB magnets. Further BNL welded the skin directly to the iron yoke whereas in MQXB magnets the skin is welded to 304L stainless steel backing strip. Its clear from Fig. 4 that GMAW process might not produce the adequate weld toughness unless tightly controlled in terms of the ferrite content and oxide inclusions.

## **(b) Mechanical Testing**

### Tensile Tests:

Uniaxial tensile testing on welds at 300, 77 and 4 K are to be conducted to determine the yield strength and the ultimate tensile strength of the weldments. These type of tests are well characterized at all temperatures. As per ASME Pressure Vessel Code, Division 1 (in particular QW-153), weld specimens must have an ultimate strength not less than the minimum specified strength of the base material. For 304 stainless steel (the base metal), Table UHA (of ASME Pressure Vessel Code, Division 1) gives a minimum required tensile strength of 80 ksi or 550 MPa. Hence the tensile strength of the welds should be not less than 550 MPa

### Charpy Impact Tests:

Per UG-84, welded specimens must have a Charpy impact energy not less than that of the base material. For a minimum tensile strength of 80 ksi, the required average impact energy of three samples is 20 ft lb (= 27.12 J) with a minimum impact energy of any one specimen of 15 ft lb (= 20.34 J). Note that these values are for standard specimens with a thickness of 0.394 inch as per Table B.2 (UG-84 (c4a)). ASME also requires that the Charpy impact tests be performed at the operating temperature. However ASTM E23-96

(the regulatory body that provides the notched bar impact test standard) restricts the temperature for cryogenic testing to a lower limit of 77K. This is based on the analysis / test results by Tobler et al. [6] on Charpy impact tests near absolute zero. They showed that there is no significant difference in the final temperature of the specimen near the crack due to the adiabatic heating for initial specimen temperatures of 4 or 77 K. Note that this is also true for tests performed with the specimen in the liquid helium bath during testing. Hence the absorbed energy for a given steel must be very similar despite the two different initial test temperatures. So we have decided to conduct the Charpy tests at 300 and 77K

Fracture Toughness Tests:

Since Charpy impact tests below 77 K are questionable, fracture toughness tests were considered necessary to evaluate the material at 4.2 K. Fracture toughness,  $K_{Ic}$  is defined as the resistance to the propagation of a crack in a given structural member i.e., the resistance force. For design purposes, if the stress intensity factor computed near any defect in the structural member is less than the fracture toughness then we can avoid catastrophic failures. Nakajima et al. [7] measured  $J_{Ic}$  (and estimated  $K_{Ic}$  from it) and compared with the Charpy impact energy ( $C_v$ ) data for several cryogenic steels. In general,  $C_v$  increased with  $J_{Ic}$ , but the data for individual alloys did not show a perfect one-to-one correlation. This is to be expected as the two tests do not measure exactly the same material properties: the Charpy test involves fracture initiation as well as propagation from a notch, whereas the  $K_{Ic}$  or  $J_{Ic}$  tests pertain to initiation only.

ASTM has proposed different test methods for measuring fracture toughness for materials that exhibit different types of fracture behavior. E 399-90 is a standard method for measuring plan-strain fracture toughness,  $K_{Ic}$ . Plane-strain refers to conditions of maximum constraint, i.e., generally thick plates and deep cracks. E 1737-96 is a standard method for J-integral characterization of fracture toughness,  $J_{Ic}$ . The path-independent J-integral proposed by Rice [8] is a method of characterizing the stress-strain field at the tip of a crack by an integral path taken sufficiently far from the crack tip to be analyzed elastically, and then substituted for an inelastic region close to the crack-tip region. However, in a plane strain linear-elastic regime,

$$K_{Ic} = \sqrt{\frac{E J_{Ic}}{1-\nu^2}} \quad (1)$$

where  $E$  is the Young's modulus and  $\nu$  is the Poisson's ratio. The J-integral values measured by this test method characterize the toughness of ductile materials that lack sufficient size and thickness to be tested for  $K_{Ic}$  in accordance with the requirements of Test Method E 399. Note that in E 399, fracture is sudden, resulting in unstable brittle fracture with little or no deformation. However, in E 1737-96, behavior is non-linear elastic-plastic with or without stable crack extension. Since the specimen sizes in our case are small and might exhibit elastic-plastic behavior, we are proposing to conduct  $J_{Ic}$  tests and estimate  $K_{Ic}$  from these values.

With this information, we are now going to analyze the MQXB longitudinal welds in terms of the required fracture toughness and the level of inspection needed. We will also investigate if the chosen filler material (308 L) and weld process (GTAW) meets these requirements.

### **3.0 FRACTURE ANALYSIS: TO DETERMINE THE REQUIRED $K_{Ic}$**

#### **(a) Through-Thickness-Yielding Criterion:**

Through-thickness-yielding criterion is based on the requirement that in the presence of a large sharp crack in a large plate, through thickness yielding should occur before fracture. This criterion is based qualitatively on two observations [9]: First, increasing the design stress in a particular application results in more stored energy in a structure. This higher amount of stored elastic energy means that the fracture toughness of the steel also should be increased to have the same degree of safety against fracture as a structure with a lower working stress and lower stored energy. Note that it is the stored energy available that propagates a crack. Second, increasing plate thickness promotes a more severe state of stress, plane strain. Thus a higher level of fracture toughness is required to obtain the same level of performance in thick plates as would be obtained in thin plates.

By using linear-elastic fracture mechanics, a fracture toughness criterion for steels to obtain through-thickness yielding before fracture was developed in terms of yield strength and plate thickness as follows [9]:

$$K_c = \sigma_y \sqrt{B} \text{ for } B \leq 50 \text{ mm} \quad (2)$$

where  $\sigma_y$  is the yield strength of the material and B is the plate thickness. In our case, B = thickness of the skin = 8 mm and  $\sigma_y$  (308 L) = 650 MPa at 4 K. Therefore required toughness to satisfy through-thickness criterion is:

$$K_c = 58.1 \text{ MPa} \sqrt{\text{m}} \quad (3)$$

#### **(b) Leak-Before-Break Criterion:**

The leak-before-break criterion is used to estimate the necessary fracture toughness so that a surface crack could grow through the wall and the vessel "leaks" before fracture. That is, the critical crack size at the design stress level of a material meeting this criterion would be greater than the wall thickness of the vessels so that the mode of failure would be leaking rather than fracture.

In the leak-before-break criterion, the depth of the surface crack, a, is set equal to the plate thickness, B. The plane-strain-fracture toughness required to satisfy this criterion is then given as [9]:

$$\frac{\pi \sigma^2}{1 - \frac{1}{2} \left( \frac{\sigma}{\sigma_y} \right)^2} = \frac{K_{Ic}^2}{B} \left[ 1 + 1.4 \left( \frac{K_{Ic}^4}{B^2 \sigma_y^4} \right) \right] \quad (4)$$

where,  $\sigma$  is the nominal design stress,  $\sigma_y$  is the yield strength of the material. Fig. 5 shows the variation of fracture toughness with applied stress. Note that as the applied stress increases,  $K_{Ic}$  required to satisfy this criterion also increases. For the critical situation of  $\sigma = \sigma_y$ , the criterion reduces to

$$\frac{1.4 K_{Ic}^6}{B^3 \sigma_y^4} + \frac{K_{Ic}^2}{B} = 2\pi \sigma_y^2 \quad (5)$$

Substituting for B (8 mm) and  $\sigma_y$  (650 MPa) we get:

$$K_{Ic} = 71.3 \text{ MPa} \sqrt{\text{m}} \quad (6)$$

Equation 6 gives the maximum toughness required to satisfy this criterion. In our case the applied stress is on the order of 300 MPa, and from Fig. 5 the required toughness to satisfy the criterion is about 42 MPa  $\sqrt{\text{m}}$ .

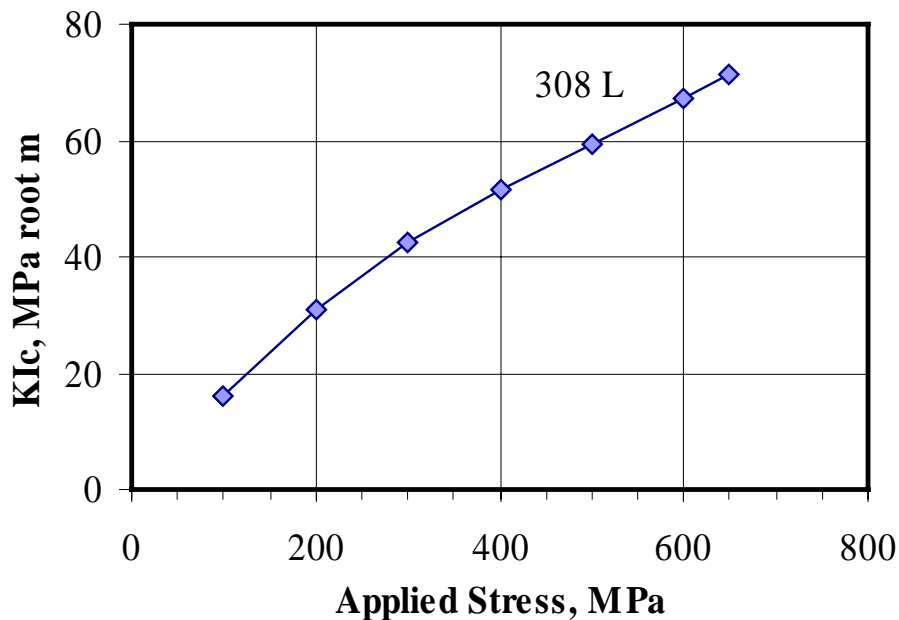


**Figure 5:** Variation of required  $K_{Ic}$  with applied stress to satisfy the leak-before-break criterion.

**(c) Critical Crack Size for a Surface Crack:**

The equation for  $K_{Ic}$  for a surface crack (as shown in Fig. 6) is given as follows [9]:

$$K_{Ic} = 1.12 \sigma \sqrt{\frac{\pi a}{Q}} M_K \quad (7)$$

where,

$$Q = \left[ \phi_o - \left( 0.212 \left( \frac{\sigma}{\sigma_y} \right)^2 \right) \right] \quad (8)$$

$$\phi_o = \int_0^{\frac{\pi}{2}} \sqrt{1 - \left( \frac{c^2 - a^2}{c^2} \right) \sin^2 \theta} d\theta \quad (9)$$

$$M_K = 1.0 + 1.2 \left( \frac{a}{B} - 0.5 \right) \quad (10)$$

$a$  = depth of the crack

$2c$  = length of the crack

$B$  = thickness of the skin

$\sigma_y$  = yield strength of the material

$\sigma$  = applied stress

$Q$  = Flaw shape Parameter

$\phi_o$  = Complete Elliptical Integral of second kind

$M_K$  = Magnification factor for deep flaws

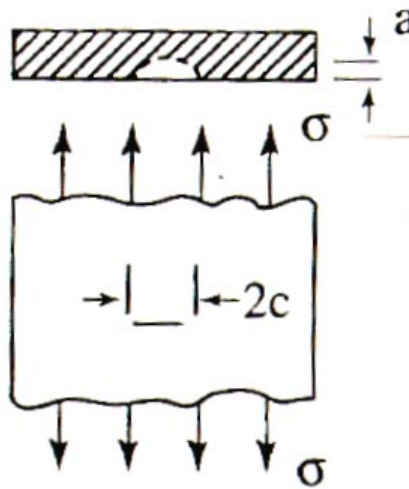


**Figure 6:** Schematic of a surface crack.

The variation of stress intensity factor,  $K_I$  with depth of the surface crack for various crack lengths is shown in the Fig. 7. Note that the maximum depth of the crack is equal to the thickness of the skin, 8 mm. As the length or depth of the crack increases, the required fracture toughness of the material increases as the stress intensity near the crack tip increases. Fig. 7 is shown for an applied stress of 200 MPa and for crack lengths ranging from 25 times the depth of the crack to 0.5 times the depth of the crack. The variation of stress intensity factor with half length of the surface crack for various crack depths and applied stress is shown in the Fig. 8. Note that as the applied stress increases from 200 to 300 MPa, the required fracture toughness of the material jumps from about 60 to 85 MPa  $\sqrt{m}$ . For larger crack lengths,  $K_I$  approaches to an asymptotic value.

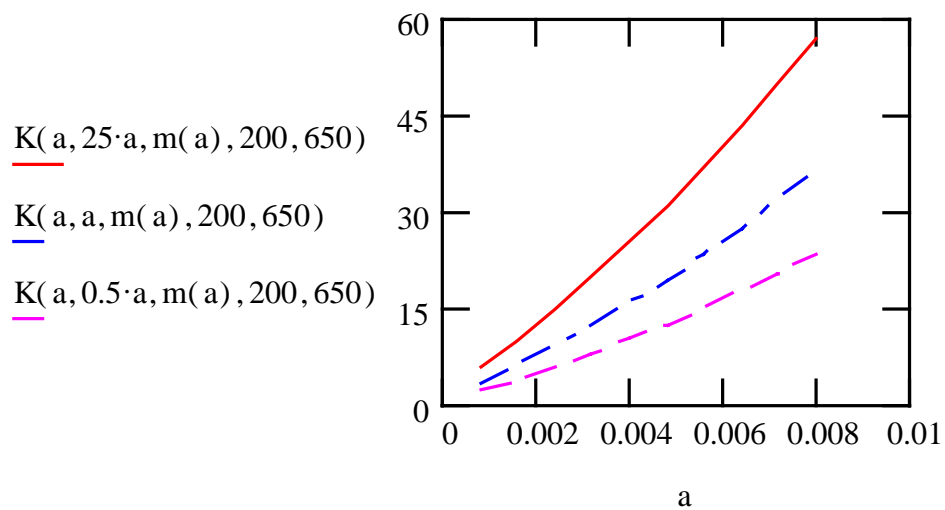


**Figure 7:** Variation of  $K$  with depth of the surface crack.

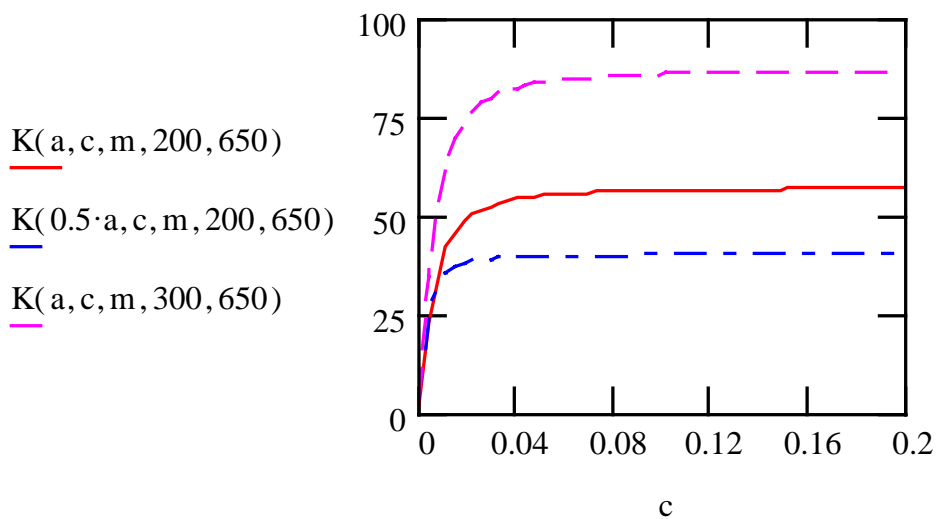


**Figure 8:** Variation of  $K$  with half length of the surface crack

So for an applied stress of 300 MPa, depth of the crack = skin thickness, the maximum stress intensity near a very large crack, or the minimum fracture toughness required for the material with this type of a crack is:

$$K_{Ic} = 85 \text{ MPa}\sqrt{\text{m}} \quad (11)$$

**(d) Required Fracture Toughness:**

Equations 3, 6 and 11 shows the required  $K_{Ic}$  for different criteria. Hence to satisfy all of them, we require a material with fracture toughness such that:

$$K_{Ic} \geq 85 \text{ MPa}\sqrt{\text{m}} \quad (12)$$

#### 4.0 CHOOSE MATERIAL AND WELD PROCESS TO OBTAIN REQUIRED $K_{Ic}$

Tobler et al. [10] obtained strength-toughness relationship for various austenitic steel welds at 4K. Fig. 9 shows their test results where the yield strength versus fracture toughness for type 308 L and 316 L are plotted. Note the scatter in the data is due to different weld materials and weld processes. The only data point with GTAW weld process is shown in the figure.

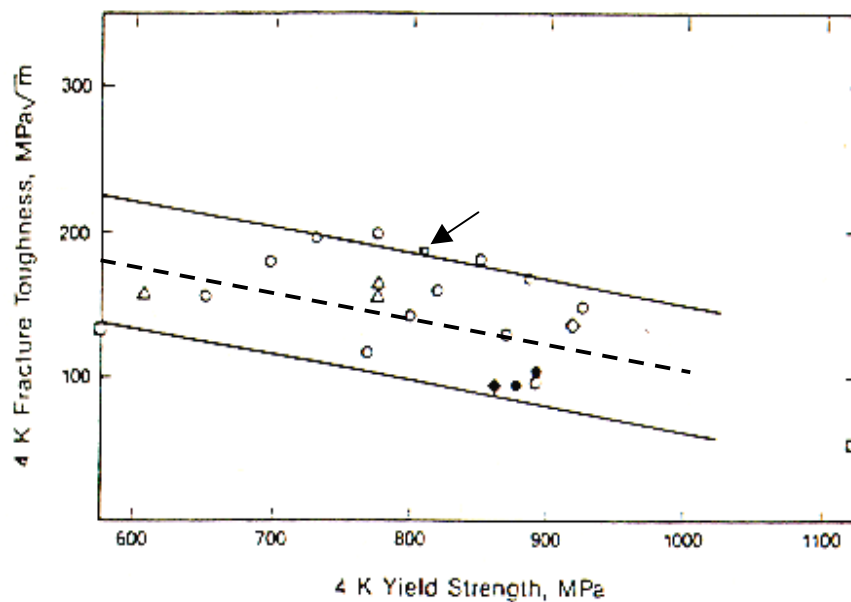


**Figure 9:** Fracture toughness versus tensile yield strength at 4K.

Empirical relationship (the dashed line) gives,

$$K_{Ic} = 270 - 0.16 \sigma_y \quad (13)$$

For 308 L welds,  $\sigma_y = 650$  MPa at 4 K, therefore,

$$K_{Ic}(308L) = 166 \text{ MPa} \sqrt{\text{m}} \quad (14)$$

Further Fig. 4 shows that GTAW welds can meet the ASME requirement quite safely even with a relatively high ferrite content. Preliminary analysis [11] on the present HGQ welds showed a ferrite content of about 5 to 8 % in the welds similar to that found by Kim et al. [5] with GTAW process and 308 L filler material. They also measured the Charpy impact energy of 53 J for 308 L with GTAW. A reasonable correlation between  $K_{Ic}$  and Charpy impact energy,  $C_v$  for steels with  $K_{Ic}$  ranging from 87 to 246 ksi $\sqrt{\text{in}}$  and  $C_v$  values ranging from 16 to 89 ft-lb is given as\* [9]:

$$\left( \frac{K_{Ic}}{\sigma_y} \right)^2 = \frac{5}{\sigma_y} \left( C_v - \frac{\sigma_y}{20} \right) \quad (15)$$

where  $K_{Ic}$  is in ksi $\sqrt{\text{in}}$ .,  $\sigma_y$  is in ksi and  $C_v$  is in ft-lb $^{\$}$ . Substituting  $\sigma_y (= 650 \text{ MPa} = 94.32 \text{ ksi})$  and  $C_v (53 \text{ J} = 39.1 \text{ ft-lb})$  we get,

$$K_{Ic}(308L) \approx 128 \text{ ksi} \sqrt{\text{in}} = 140 \text{ MPa} \sqrt{\text{m}} \quad (16)$$

**Equations 14 and 16 show that with 308 L as a filler material, we can satisfy the required fracture toughness criteria using GTAW weld process.**

\* The relationship between  $K_{Ic}$  and  $C_v$  should be used with caution as there is no perfect one-to-one correlation between them for all steels [7].

$\$$  1 ft-lb = 1.356 J

1 ksi $\sqrt{\text{in}}$  = 1.099 MPa $\sqrt{\text{m}}$

## 5.0 LEVEL OF INSPECTION ON WELDMENTS

### (a) Critical Crack Size for Through Thickness Crack:

The relationship between the fracture toughness, applied stress and the crack length for a through thickness crack is given as [9]:

$$K_{Ic} = \sigma \sqrt{\pi a} \quad (17)$$

where,  $2a$  is the length of the crack and  $\sigma$  is the applied stress. Fig. 10 shows the schematic of a through thickness crack and Fig. 11 shows the variation of crack length with fracture toughness. Note that for a fracture toughness of  $166 \text{ MPa}\sqrt{\text{m}}$  and an applied stress of  $300 \text{ MPa}$ , we need to detect a through thickness crack which is about  $200 \text{ mm}$  long.

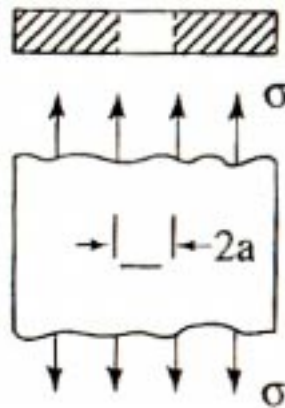


**Figure 10:** Schematic of through thickness crack.

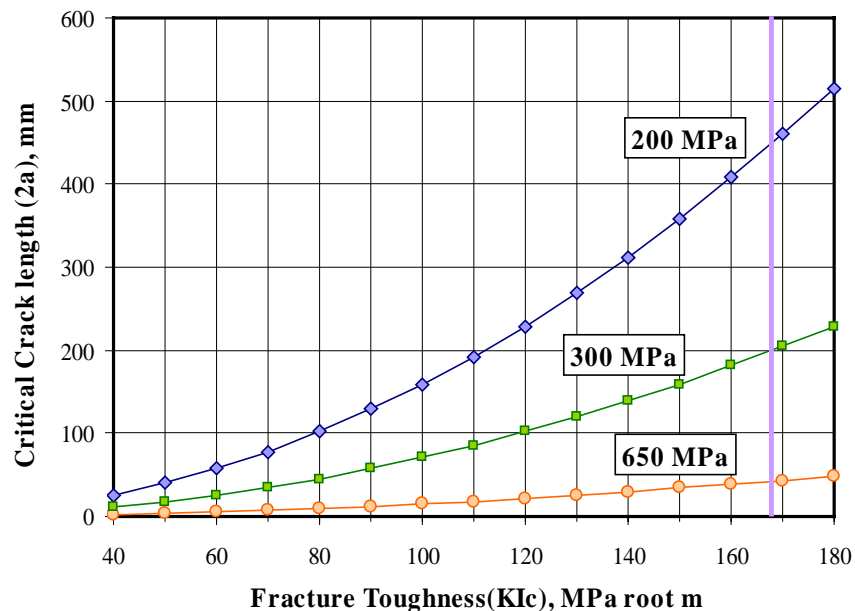


**Figure 11:** Variation of critical crack length with fracture toughness.

**(b) Fatigue Crack Growth of a Surface Crack:**

An empirical relationship for the fatigue-crack propagation behavior in austenitic steels is given as [9]:

$$\frac{da}{dN} = 3.0 \times 10^{-10} (\Delta K_I)^{3.25} \quad (18)$$

where  $a$  is the crack size in inches,  $\Delta K_I$  is the stress-intensity-factor fluctuation in  $\text{ksi}\sqrt{\text{in}}$  and  $N$  is the number of cycles. For a surface crack with a constant stress range of  $\Delta\sigma$ , the stress-intensity-factor fluctuation is given as:

$$\Delta K_I = 1.12 \Delta\sigma \sqrt{\frac{\pi a_{\text{avg}}}{Q}} M_K \quad (19)$$

where  $a_{\text{avg}}$  is the average crack size between the two crack increments;  $Q$  and  $M_K$  are defined in the previous section. Lets denote  $a_0$  to be the initial flaw size and  $\Delta a$  to be increment of crack extension from  $a_0$ .

For MQXB magnets,  $\Delta\sigma = 200 \text{ MPa}$ ; assume a initial flaw size,  $a_0$  of 0.8 mm and 1.6 mm with a increment of crack extension  $\Delta a$  to be 0.08 mm; and for simplicity assume  $c = a$  (ie., circular inclusion). Note that the maximum allowed flaw size is equal to the thickness of the skin, 8 mm. With these values we can compute  $\Delta K_I$  using Eq. 19 and then  $N$  from Eq. 18. Fig. 12 shows these results.

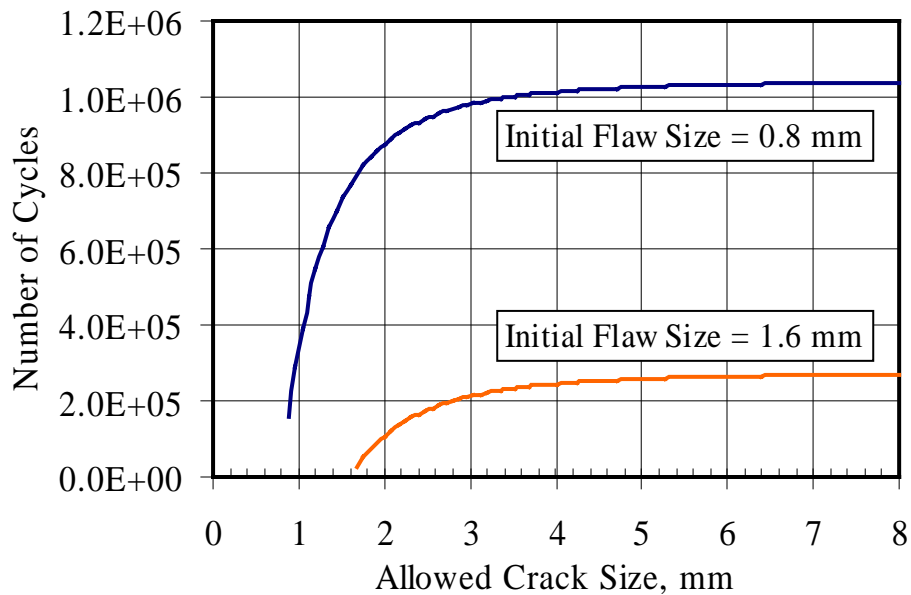


**Fig. 12:** Number of cycles to failure due to fatigue crack propagation.

A initial flaw size of 1.6 mm is considered because if we miss a filler pass during welding we would then leave a void of this size. With this initial flaw size the number of cycles for failure is about  $3.0 \times 10^5$ . Note that these magnets will see about 25 cycles in their life time. If we were to calculate the initial flaw size for the magnet to fail in 25 cycles, it comes to approximately 537 mm.

The empirical relationship used in Eq. 18 was originally derived for austenitic steels in room temperature air environment. However S-N curves (i.e., peak stress versus fatigue life) generated by Siewert et al. [12] for notched weld specimens (316L) showed similar behavior at 298 and 4 K. If we extrapolate their results for a peak stress of 300 MPa, we get a fatigue life of about  $1.5 \times 10^5$  cycles at 4 K and  $2 \times 10^5$  cycles at 298 K. Note that their last data point was for a peak stress of 400 MPa which yielded a fatigue life of  $4 \times 10^4$  cycles at 4 K.

**It appears that for these materials and process, a level of inspection consistent with finding through thickness cracks or surface cracks greater than 200 mm long is sufficient to prevent catastrophic failure.**

## 6.0 FUTURE WORK: EXPERIMENTAL VERIFICATION

A 2 m long mechanical model (skin-yoke assembly without collared coil) was recently welded to perform mechanical tests. Note that the welding process used to weld this mechanical model is exactly the same as would be done for the final MQXB magnets. The following tests have been proposed after various consultations with NIST [13]:

Type of Test	Material	Temperature	Number of tests
Tension	308 L	300 K	2
Tension	308 L	4.2 K	2
Charpy Impact	308 L	300 K	3
Charpy Impact	308 L	77 K	3
Charpy Impact	HAZ	77 K	3
Fracture Toughness	308 L	300 K	3
Fracture Toughness	308 L	4.2 K	3
Fracture Toughness	HAZ	4.2 K	3
Fatigue Test (notched specimen)	308 L	4.2 K	3
Fracture Toughness	304 (base metal)	4.2 K	3

**Table 1:** Matrix of experiments proposed to test the weldments.

Tension tests gives us the strength of the weldments. This is not very critical for MQXB magnets, as the skin is not stressed heavily unlike in LHC or RHIC dipoles. Tobler et al. [10] showed that fracture toughness is inversely proportional to the strength. So Charpy impact tests and fracture toughness tests will show us whether the material has the required toughness to prevent catastrophic failures. Both Charpy and plane-strain fracture toughness

tests are proposed as the former is questionable below 77K [6]. Fatigue tests with a notched specimen will give us the number of cycles before the welds fail. Note from the analysis it was clear that fatigue was not an issue here as the magnets are expected to undergo only 25 cycles.

We have also sent out sections from earlier mechanical model to get our welders ASME certified and to measure the inclusion size and ferrite content in the welds [11].

## REFERENCES

1. M. Bajko, P. Fessia, and D. Perini, "FEM Computations concerning the effect of friction in two LHC main dipole structures", presented in *MT16*, 1999.
2. S.F. Kane et al, "Welding Consumable Selection for a Cryogenic (4K) Application", BNL-62469 (AD/RHIC-137) Informal Report, November 1995; and "Fracture Toughness Requirements for RHIC Cryogenic Design", AD/RHIC/RD-40, May 1992.
3. T.A. Siewert and C.N. McCowan, "Joining of Austenitic Stainless Steels for Cryogenic Applications", *Advances in Cryogenic Engineering*, Vol. 38, 1992, pg. 109.
4. C.N. McCowan and T.A. Siewert, "Fracture toughness of 316 L stainless steel welds with varying inclusion contents at 4 K", *Advances in Cryogenic Engineering*, Vol. 36, 1990, pg. 1331.
5. J.H. Kim, et al., "Effect of Oxygen Content on Cryogenic Toughness of Austenitic Stainless Steel Weld Metal", *Advances in Cryogenic Engineering*, Vol. 36, 1990, pg. 1339.
6. R.L. Tobler et al., "Charpy Impact Tests Near Absolute Zero", *J. Testing and Evaluation*, Vol. 19, No. 1, 1991, pg. 34.
7. H. Nakajima et al., "Fracture toughness of newly developed structural materials for superconducting coils of fusion experimental reactor", *Advances in Cryogenic Engineering*, Vol. 32, 1986, pg. 347.
8. J.A. Rice, "A path independent integral and the approximate analysis of strain concentration by notches and cracks", *J. Applied Mechanics*, Vol. 35, 1968.
9. J.M. Barsom and S.T. Rolfe, "Fracture and Fatigue Control in Structures", ASTM, 1999.
10. R.L. Tobler, T.A. Siewert, and H.I. McHenry, "Strength-toughness relationship for austenitic stainless steel welds at 4K", *Cryogenics*, Vol. 26, July 1986, p392.

11. D.R. Chichili, J. Kerby et al., "MQXB Longitudinal Weld Analysis: Mechanical Testing of Weld Samples", to be published.
12. T.A. Siewert, C.N. McCowan and D.P. Vigliotti, "Cryogenic material properties of stainless steel tube-to-flange welds", *Cryogenics*, Vol. 30, April 1990, p356.
13. Various private communications with T. Siewert, NIST.